

# STUDY ON HEAT TRANSFER CHARACTERISTICS OF Z-TYPE PARALLEL MULTI-BRANCH PIPE GROUP

Yue XU<sup>1</sup>, Qipeng LI<sup>1</sup>, Yu WANG<sup>\*1</sup>, Wenhui TANG<sup>2</sup>, Asfandiyar Khan DAWAR<sup>1</sup>, Risto KOSONEN<sup>3</sup>,  
Yingying ZHANG<sup>1</sup> and Nianyong ZHOU<sup>4</sup>

<sup>\*1</sup>Department of HVAC Engineering, College of Urban Construction, Nanjing Tech University, Nanjing 211816, P. R. China

<sup>2</sup> China Shipbuilding Corporation Eighth Research Institute, Nanjing 211153, P. R. China

<sup>3</sup>Department of Mechanical Engineering, Aalto University, Espoo 021050, Finland

<sup>4</sup>School of Urban Construction, Changzhou University, Changzhou 213164, P. R. China

\* Corresponding author; E-mail: [yu-wang@njtech.edu.cn](mailto:yu-wang@njtech.edu.cn)

*Z-type parallel multi-branch pipe groups are widely utilized to deliver fluid in cooling high-power electronic equipment. Computational Fluid Dynamics (CFD) software is commonly used to perform numerical simulations of these systems. This study examines the effects of varying inlet flow rates, branch pipe diameters, and main pipe diameters on flow characteristics and heat transfer. The flow deviation coefficient and temperature distribution were used to assess the flow uniformity in branch pipes and the heat transfer efficiency of cold plates. The findings reveal that increasing the inlet flow rate enhances flow inhomogeneity but decreases the overall temperature of the cold plate. Similarly, increasing the branch pipe diameter strengthens flow inhomogeneity without significantly affecting the cold plate's temperature distribution. Conversely, increasing the main pipe diameter exacerbates the uneven flow distribution and results in more local hot spots on the cold plate. Based on these simulation results, an optimized design for Z-type parallel multi-branch pipe systems can be developed to improve flow uniformity and heat transfer efficiency.*

*Keywords: Parallel multi-branch pipes, Flow uniformity, Temperature distribution, Heat transfer effect, Numerical simulation*

## 1. Introduction

With the rapid development of radar technology, traditional air cooling technology can no longer meet the heat dissipation requirements of electronic components in high-power radar systems. The cold-plate liquid-cooling technology possesses extreme advantages of higher thermal conductivity, smaller dimension and easier to integrate, to have wider application in high-power radar cooling systems. The Z-type parallel multi-branch pipe group is a typical flow distribution device in the radar cooling system, usually composed of a diverter header, a combiner header, and several branch pipes. The resistance characteristics and flow channel design in Z-type pipe group guarantee the appropriate flow rate of coolant, and make sure to

exchange heat between cold plates and cooling liquid quickly channel design in Z-type pipe group guarantee to avoid safety issues. Therefore, studying the flow characteristics of cooling liquid in Z-type parallel pipe group means significantly for ensuring radar systems work.

Before conducting research on the Z - type multi - branch cold plate, we searched through various literatures to understand the development history of the cold plate and the current research level of cold plates. Moreover, we carried out detailed research work using a large number of cold plates available on the market. Multi - branch cold plates have become the mainstream type in the market. It was found that flow imbalance occurs in all types of multi - branch cold plates, which will lead to a poor cooling effect of the cold plate and make it difficult to achieve the designed cooling standards. Since the  $2 \times 7$  multi - branch cold plate is a fundamental type of multi - branch cold plate, studying the reasons for the uneven flow distribution in the  $2 \times 7$  multi - branch cold plate will be beneficial to the design research of complex multi - branch cold plates.

The phenomenon of uneven flow distribution is an inherent attribute on the Z-type parallel pipe group. At present, research on the flow characteristics of parallel multi-branch pipes mainly focuses on flow distribution characteristics and the influencing factors which are mainly divided into two categories: structural parameters and flow states.

Kubo and Ueda [1] studied the flow distribution of parallel pipelines under different branch diameters and found that the smaller the branch diameter, the greater the flow rate resistance of the pipeline, and the better the uniformity of flow distribution. Ahn *et al.* [2] studied the effects of changes in branch length and quantity on flow distribution, and the results showed that the influence of branch length on flow resistance and flow distribution was relatively smaller. Lee [3] conducted research on the insertion depth of branch pipes, and found that adjusting the insertion depth of branch pipes can improve the flow distribution performance of pipelines. Zhu [4] compared the distribution characteristics of traditional headers and headers with added flute shaped pipes, and found that the distribution characteristics of the header system were greatly improved with flute shaped pipes.

Chen [5] found that the influence of structural parameters is mainly achieved by changing the pipe diameter, length, cross-sectional shape, cross-sectional ratio, and other aspects. If the connection methods between the main pipe and the branch pipe are modified, changing the shape of the branch pipe mouth, adding porous components and other transforming structure methods could be the optional modification methods.

As a result of the complexity of fluid flow, it is difficult to find the exact solution in hydrodynamics, using computational fluid dynamics (CFD) software to simulate the fluid flow in parallel multi-branch pipe group has become the main method. Griffini and Gavriilidis, Kim *et al.* [6-7] used numerical simulation to study the flow distribution under different main pipe lengths. The results showed that the flow distribution performance of the parallel pipeline was better with the increase of main pipe length. Acrivos *et al.* [8] established a one-dimensional flow equation for the flow rate and distribution of single-phase fluid in the pipe. The experimental and calculation results showed that the change of pressure distribution in the pipe was determined by the friction loss caused by flow and the change of fluid momentum caused by division. Amador *et al.* [9] simulated different main pipe cross-sectional area sizes and main pipe inlet shapes by simulation software and found that increasing or decreasing the main pipe cross-sectional area along the flow direction can increase the fluid distribution uniformity. Lee and Sang [10] studied the insertion depth of branch pipe and main pipe, and found that by adjusting the insertion depth of branch pipe can improve the uniformity of pipeline flow distribution to a certain extent. Kim and Han [11] investigated the impact of

varying insertion depths of branch pipes into the main pipe on flow distribution. Their results indicate that when the branch pipe is not inserted deeply, the distance from the inlet to the branch pipe in the main pipeline is greater. As the insertion depth increases, resistance loss in the diverging pipe causes a more pronounced uneven distribution of fluid flow.

Fang *et al.* [12] investigated the effects of coolant flow rate, heat flow density increment, and number of channels on the transient thermal performance of the cold plate, and the results showed that an increase in coolant flow rate by a certain amount of flow rate would result in an excessive temperature deviation of the cold plate, and that an increase in the heat flow density and an increase in the number of channels would result in an increase in the cold plate's average temperature and temperature deviation. Shen and Gao [13] studied the effect of refrigerant mass flux on the cold plate, and the results showed that the refrigerant mass flux is the optimal solution for thermal management of the cold plate. Hosseini *et al.* [14] investigated the causes of high-cycle thermal fatigue in cooling systems, studying fluent variations at the T-joint location, and showed that the angle and velocity at the elbow affect the thermal fatigue of the cold plate. Gong *et al.* [15] used numerical simulation to study the effect of microchannels on the heat transfer effect of the cold plate, and the results show that the heat transfer effect of the cold plate of different structures is different, and the width of the microchannel will affect the temperature uniformity of the cold plate. Sharma *et al.* [16] investigated the flow distribution problem present in microreactors and showed that the problem of flow distribution uniformity was improved by changing the model structure and other methods.

In summary, most efforts to improve the flow rate characteristics of parallel multi-branch pipes have focused on local performance optimization, yielding limited improvements. This paper analyzes the flow and heat transfer characteristics of a cooling system for high-power radar using numerical simulations. Combining single-factor conditions with orthogonal tests, we designed an orthogonal table based on single-factor test analysis. We comprehensively examined the effects of three parameters—inlet flow, branch pipe diameter, and main pipe diameter—on flow uniformity and heat transfer efficiency of the cold plate. Comparing the results of the orthogonal optimal structure combination with single-factor tests, we demonstrate that the optimal parameter combination aligns with the single-factor trends.

## 2. Physical model, mathematical model and boundary conditions

### 2.1. Physical model

Figure 1 shows the three-dimensional physical model of  $2 \times 7$  Z-type parallel multi-branch pipe group.

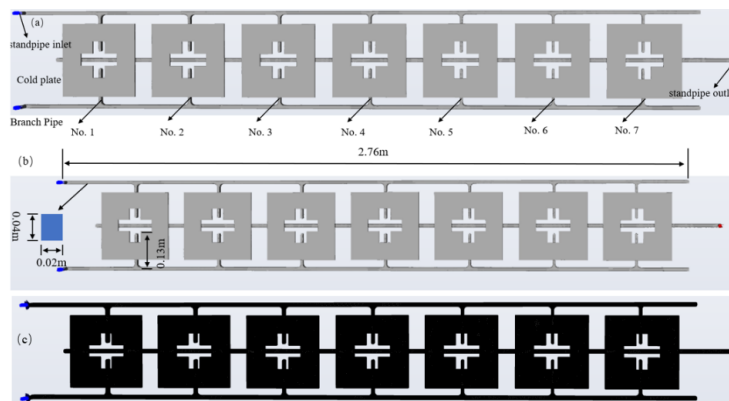


**Fig. 1. Three-dimensional model size and meshing of  $2 \times 7$  Z type parallel multi-branch pipe**

The diverter header is located on the left and right sides, with a header length of 2.76 m and a section dimension of  $0.02 \times 0.04$  m. The combiner header is located in the middle of the diverter header on both sides with same dimension as the diverter header, equidistant from left and right sides. Seven branch pipes with the same dimension are distributed on the one side of the diverter header, and the branches are equally spaced from each other, with the length of 0.13 m. Seven cold plates are connected to the surfaces of the seven branch pipes on the left and right sides and are arranged equidistant.

A three-dimensional physical model of 2×7 Z parallel multi-branch pipe is shown in Fig. 1 ( a ). From left to right, the cold plate number is 1-7. Fig. 1 ( b ) is the size introduction diagram of the model, and Fig. 1 ( c ) is the model grid division diagram.

In the parallel pipe group applied in plate liquid cooling, the coolant flows into the cold plate through the branch pipes and exchanges heat with the heating electronic devices outside the cold plate, and then the heated coolant flows out of the pipe group through combiner header.

## 2.2. Mathematical model

The flow and heat transfer of coolant in the pipeline are described by mass conservation equation, momentum conservation equation and energy conservation equation, where:

Mass conservation equation: The increase in the mass of a fluid micro-element per unit time is equal to the net mass flowing into the micro-element during the same period of time.

$$\frac{\partial \rho}{\partial t} + \frac{\partial(\rho u)}{\partial x} + \frac{\partial(\rho v)}{\partial y} + \frac{\partial(\rho w)}{\partial z} = 0 \quad (1)$$

$$\frac{\partial a_x}{\partial x} + \frac{\partial a_y}{\partial y} + \frac{\partial a_z}{\partial z} = \text{div}(a) \quad (2)$$

$$\frac{\partial \rho}{\partial t} + \text{div}(\rho U) = 0 \quad (3)$$

In the equation,  $\rho$  is the density of the fluid,  $\text{kg} / \text{m}^3$ ,  $t$  is time,  $s$ ;  $u$  is the velocity vector;  $u, v, w$  are the velocity components of the fluid in the  $x, y, z$  directions at time  $t$ .

Momentum conservation equation: The specific expression equation is shown in Eq. 4、Eq. 5、Eq. 6 :

$$\frac{\partial(\rho u)}{\partial t} + \text{div}(\rho u U) = \text{div}(\mu \square \text{grad} u) - \frac{\partial p}{\partial x} + S_u \quad (4)$$

$$\frac{\partial(\rho v)}{\partial t} + \text{div}(\rho v U) = \text{div}(\mu \square \text{grad} v) - \frac{\partial p}{\partial y} + S_v \quad (5)$$

$$\frac{\partial(\rho w)}{\partial t} + \text{div}(\rho w U) = \text{div}(\mu \square \text{grad} w) - \frac{\partial p}{\partial z} + S_w \quad (6)$$

Energy conservation equation: The heat transfer between the coolant and the cold plate needs to be simulated, so the energy conservation equation needs to be considered. The equation is shown in Eq. 7 :

$$\frac{\partial(\rho T)}{\partial t} + \text{div}(\rho UT) = \text{div}\left(\frac{k}{c_p} \text{grad}T\right) + S_T \quad (7)$$

Where  $T$  is the temperature, K;  $C_p$  is the specific heat capacity of the fluid, J/(kg·K);  $S_T$  represents the dissipation term of the fluid.

### 2.3. Boundary conditions

ANSYS Fluent software contains three typical k-epsilon models: Standard k-ε, RNG k-ε and Realizable k-ε. In this paper, the physical model is mainly composed of rectangular channels and the flow states mainly involve the large curvature flow and shear flow. Therefore, the Realizable k-ε model is selected as the turbulent flow model in Fluent settings.

The fluid in simulation is set as incompressible single-phase flow, isotropic, and the physical parameters keep constant. The boundary conditions are set as shown in Tab. 1.

In order to reduce the calculation inaccuracy caused by the insufficient mesh quality, the Enhanced Treatment is selected as the wall function and the other relevant settings are Steady calculation, SIMPLE algorithm and second order upwind. The convergence of the calculation is considered when the residual deviation of variables is less than  $10^{-4}$ .

**Table 1. Boundary conditions**

Type	Boundary conditions
Inlet	Velocity inlet
Outlet	Pressure outlet
Wall	Static non slip wall
	Adiabatic
	Roughness: Ra3.2
Cold Plates	Constant heat flux: 200 W/cm <sup>2</sup>
	Material: aluminum
	Material: aluminum
Headers	Thermal conductivity: 230 W/m.K

The coolant of radar in this paper is 65# radar cooling liquid, which mainly consists of ethylene glycol, distilled water, corrosion inhibitor and antioxidant.

The flow deviation coefficient is calculated as Eq. 8:

$$\eta_{\max} = (\eta_{L \max} - \eta_{L \min}) \quad (8)$$

In this equation,  $\eta_{\max}$  is the flow deviation coefficient.

## 3. Mesh decomposition and Grid independence test

### 3.1. Mesh decomposition

The grid quality evaluations in ANSYS Mesh software mainly include Element Quality, Skewness and so on. The Element Quality ranges from 0 (the worst) to 1 (the best), and the average value greater than 0.75 indicates excellent quality. The Skewness ranges from 0 (the best) to 1 (the worst), and the smaller the average value, the higher quality of grids.

The Element Quality and Skewness were used to evaluate the quality of the divided grids. The average value of Element Quality is 0.915, and the minimum value is greater than 0.2. In terms of Skewness, the average value of all grids is 0.23. Therefore, it can be considered that the grid quality meets the requirements of numerical simulation. Fig. 2 (a) shows the details of the meshing of a single cold plate. The meshing of the whole model is shown in Fig. 1 (c). Fig. 2 (b) shows that the model is locally refined in order to improve the quality of the mesh during the meshing process.

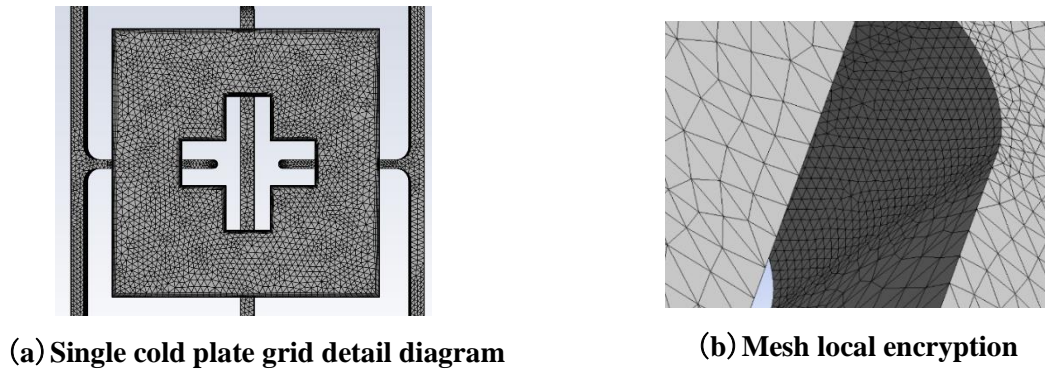


**Fig. 2. Mesh decomposition diagram**

### 3.2. Grid independence test

In order to study the dependence of numerical simulation on grids, grids with 552,282, 740,508, 975,023, 1,099,463, and 1,751,780 were selected to simulate branch flow rate under the same working conditions.

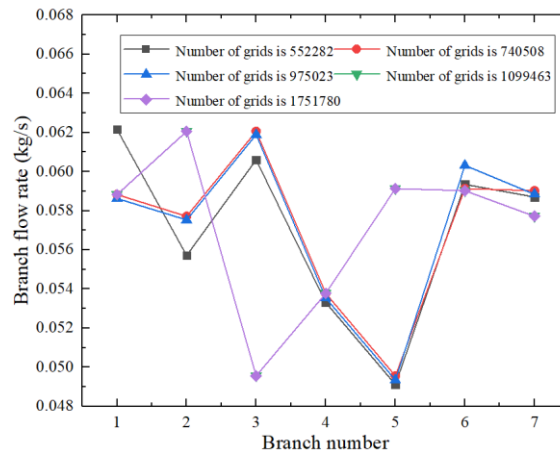


**Fig. 3. The results are verified under different grid numbers**

When the deviation of adjacent data is within 5%, it can be considered that the influence of grids number on the simulation results is acceptable.

Figure 3 shows the flow of the model with different number of grids, from which it can be found that the curves of 1,099,463 and 1,751,780 grids completely coincide, indicating that the impact of increasing grids numbers is little, and the simulation data is irrelevant to the grids number. Therefore, the minimum grids number is set as 1,099,463 in later numerical simulation.

### 3.3. Simulation validation

In order to verify the credibility of the simulation, a real model of  $2 \times 7$  parallel multi branch pipe group is established, as shown in Fig. 4. The experiment was completed in November 2023 in Department of HVAC Engineering, College of Urban Construction, Nanjing Tech University, Nanjing, China.



**Fig. 4. Schematic of the  $2 \times 7$  Z-type parallel multi-branch pipe**

The experimental system is composed of  $2 \times 7$  parallel multi-branch pipe group, liquid cooling plates and water pump, and the temperature measuring tool is K-type thermocouple. The material of the experimental model is aluminum, the thermal consumption of cold plates is 100 W, the coolant medium is R134a, and the inlet flow rate is set as 0.19 m/s. In order to get the average temperature of each cold plate, the cold plate surfaces are divided into four areas and the temperature measuring points are arranged as it shown in Fig. 5.

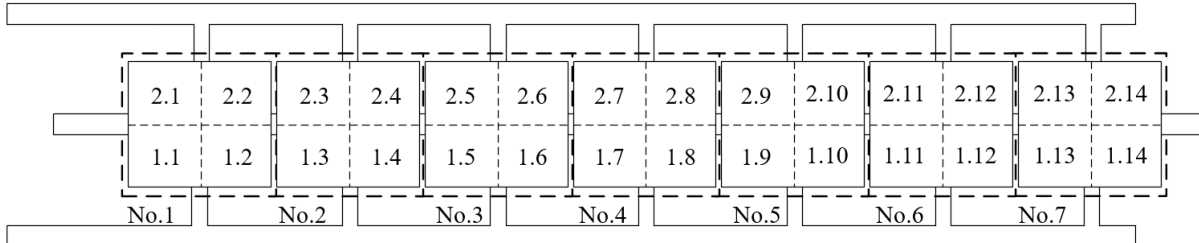


**Fig. 5. Arrangement of cold plate temperature measurement and control points**

In the numerical simulation, the fluid physical parameters, boundary conditions and other related settings are consistent with the experiment, and the Fluent settings are consistent with Section 2.3. The average surface temperatures of seven cold plates obtained by simulation were compared with the experimental values.

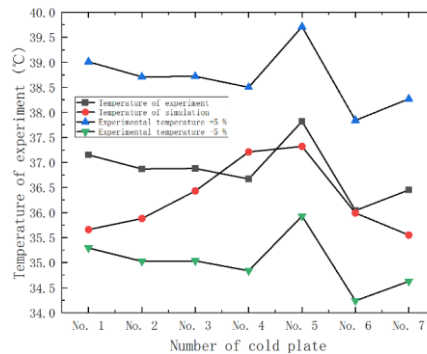


**Fig. 6. Comparison of experimental temperature and simulation temperature**

Figure 6 shows the comparison between the experimental data and the simulation data of the cold plate under the same physical parameters. It can be seen that the temperature of the seven cold plates is about 37 °C, and the simulation temperature is about 36 °C. The deviation between the experimental temperature and the simulation temperature of the same cold plate is within 1 °C, and the error between the experimental temperature and the simulation temperature is within  $\pm 5\%$ , which can verify the authenticity of the simulation results.

### 3.4. Experimental uncertainty analysis

The uncertainty of the experimental results refers to the standard uncertainty, which is divided into class A standard uncertainty and class B standard uncertainty. Class A uncertainty is the measurement column obtained from  $n$  independent repetitions of the measured value, which is the direct measurement uncertainty. Class B uncertainty cannot be determined statistically within the measurement range and is estimated mainly based on experience or other relevant information, generally only the uncertainty caused by instrument error is considered.

The sum of the squares of the Class A uncertainty component and the Class B uncertainty component is the quadratic of the standard synthetic uncertainty. The uncertainty of the experimental results is calculated from the synthetic standard uncertainty, which is given in Eq. 9:

$$U = \sqrt{\sum_{i=1}^n u_{A,i}^2 + \sum_{j=1}^n u_{B,j}^2} \quad (9)$$

Where  $u_{A,i}$  is the class A uncertainty component;  $u_{B,j}$  is the class B uncertainty component;  $n$  is the number of measurements.

The experimental data were also compared with the simulation results, and the maximum relative error for the maximum temperature was 0.6°C (2%) and the maximum relative error for the average temperature was 0.6°C (1.8%), which were found to be in good agreement, thus verifying the accuracy of the numerical simulation. The relative error due to the temperature measuring instrument is  $\pm 0.15\%$ , and the relative error due to the pump is  $\pm 5\%$ , the overall relative error of the experiment was small.

## 4. Influence of different parameters on flow uniformity and heat transfer

### 4.1. Different inlet flow rates

Five different inlet flow rates ( $Q_{inlet}$ ) are set: 0.068 kg/s, 0.274 kg/s, 0.616 kg/s, 1.164 kg/s, 1.711 kg/s and the type of inlet is mass inlet. The diameters of branch pipe ( $d$ ) and the main pipe ( $D$ ) are  $d=0.01\text{m}$  and  $D=0.015\text{ m}$ . Specially, when the inlet flow rate is 0.068 kg/s and 0.274 kg/s, the flow model in Fluent software is chosen as Laminar model, and the parameters of the rest working conditions are set as Section 2.3.

With the increase of inlet flow rate, the flow deviation coefficient of branch pipes increases at the same time, and the non-uniformity of branch pipes intensifies.

With the increase of inlet flow rate, the temperature distribution in cold plate is significantly improved, and the overall temperature of cold plates is significantly reduced. Under the same inlet flow rate, the temperature distribution of No. 1~7 cold plates is different, and the temperature on No.1 cold plate and No.7 cold plate is significantly lower than that in other cold plates.



The worst cooling effect can be indicated through the highest temperature of cold plates, and the temperature uniformity of cold plates could be shown through the average temperature and the largest temperature difference. Therefore, the highest temperature, the average temperature and the largest temperature difference on cold plates were chosen as the index of cooling effect. When analysing the temperature distribution of the different cold plates, the temperature distribution of cold plate 4 is the most unfavorable condition. Therefore, taking the No.4 cold plate as an example, the temperature distribution in No.4 cold plate under different inlet flow rates is shown in Fig. 7. Presented results are calculated by numerical simulation.

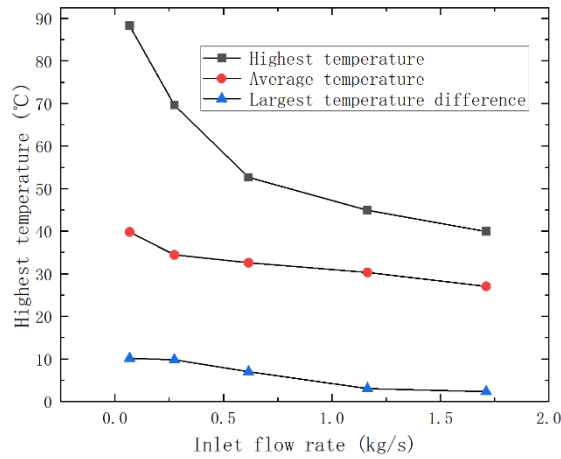


**Fig. 7. Temperature distribution of cold plate under different inlet flow rate**

According to the temperature limit for the safe operation of high-power radar below 80 °C, when the inlet flow rate is greater than 0.068 kg/s, the temperature distribution of the cold plate can meet the radar operating temperature limit. For the uniform temperature of high-power radar, the maximum temperature difference of the array panel should be controlled within 3 °C. When the inlet flow reaches 1.164 kg/s, the maximum temperature difference of the most unfavorable cold plate is within 3 °C. Considering the high-temperature limit and temperature uniformity, the minimum coolant flow rate suitable for the radar in this model is 1.164 kg / s.

Although increasing the inlet flow rate can reduce the average temperature and maximum temperature difference of the cold plate, but the fluctuation range of the average temperature of the cold plate also reaches 12 °C. The temperature fluctuation range of the cold plate is large, which will lead to the phenomenon of redundant design cooling capacity in order to meet the sufficient low-temperature cooling temperature in the actual operation, which will aggravate the energy waste. Therefore, it is necessary to comprehensively consider energy saving on the basis of meeting the heat transfer effect.

#### 4.2. Different branch pipe diameters

Five different branch pipe diameters ( $d$ ) are set: 0.01 m, 0.015 m, 0.02 m, 0.025 m, 0.03 m, and the inlet is velocity inlet. The inlet flow rate ( $Q_{inlet}$ ) and main pipe diameter ( $D$ ) are  $Q_{inlet}=1.711$  kg/s and  $D=0.015$  m.

The velocity of fluid in pipe will be reduced because of the increase of branch pipe diameter, and then will cause the resistance loss and friction dissipation decrease, while the pressure in branch pipes is affected by momentum and friction resistance, as a result the pressure in branch pipe will decrease eventually, which

will enlarge the pressure difference between inlet and outlet of the branch pipe and intensify the non-uniformity of flow distribution.

In real design, reducing the branch pipe diameter will strengthen the uniformity of flow distribution, but also the flow resistance at the branch tee will be enlarged. Therefore, the dual effects of flow uniformity and resistance loss need to be comprehensively considered in the real design process.

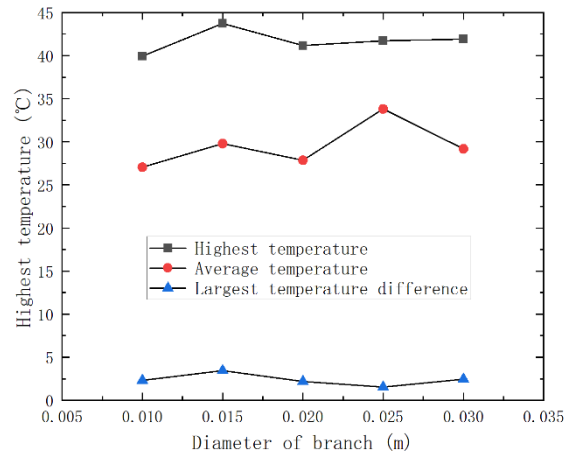


**Fig. 8. Temperature distribution of cold plate under different pipe diameters**

Comparing the temperature distribution of seven cold plates under the same pipe diameter, and it is found that No.4 ~ 6 cold plate temperature is higher than that of other cold plates, and the temperature of the No.7 cold plate is the lowest. The temperature distribution in cold plate No. 4 with different branch pipe diameters is shown as an example in Fig. 8.

It can be seen from the Fig. 8 that with the increase of branch pipe diameter, the rule of the highest temperature, largest temperature difference and average temperature variation in cold plate is unclear, and the peak value appear time is inconsistent, indicating that the increase of the branch pipe diameter has little effect on the heat transfer effect in cold plates, which is inconsistent with the influence of changing the flow state on the heat transfer of the cold plate. In general, increasing the branch pipe diameter will aggravate the flow non-uniformity of branch pipes, but the temperature distribution and local hot spot in cold plates will be improved.

When the diameter of the branch pipe increases from 0.01 m to 0.03 m, the maximum temperature of the cold plate is lower than 80 °C, which meets the high temperature operating temperature limit of the radar. When the branch pipe diameter is greater than 0.015 m, the surface temperature uniformity of the most unfavorable cold plate meets the requirement of less than 3 °C.

#### 4.3. Different main pipe diameters

In this section, five different main diameters ( $D$ ) are set: 0.015 m, 0.02 m, 0.03 m, 0.04 m, 0.05 m, and the inlet is a velocity inlet. The inlet flow ( $Q_{inlet}$ ) and branch diameter ( $d$ ) are  $Q_{inlet}=1.711$  kg/s and  $d=0.01$  m.

If the diameter of the main pipe is increased and the inlet flow rate is kept constant, the coolant flow rate will decrease according to the relationship between flow rate and flow velocity, which will weaken the turbulence intensity and make it difficult to form eddies.

As a result, the pressure difference between the inlet and outlet of the branch pipe will increase, thus exacerbating the flow inhomogeneity. Taking No.4 cold plate as an example and the temperature distribution in No.4 cold plate under different main pipe diameters is shown in Fig. 9.

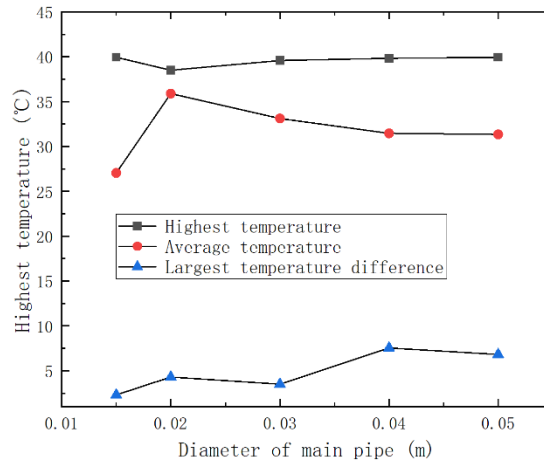


**Fig. 9. Temperature distribution of cold plate under different main pipe diameters**

#### 4.4. Orthogonal test

The comprehensive influence of inlet flow, branch pipe diameter and main pipe diameter on branch pipe flow uniformity and cold plate heat transfer efficiency can not be reflected by single-factor test, and the optimal parameter combination also can not be obtained. Therefore, it is necessary to combine simulation with orthogonal test. Therefore, five levels are set for three factors and the orthogonal table design is listed in Tab. 2. According to the orthogonal test table designed by three factors and five levels, there are 25 groups of sample points.

**Table 2. Parameters of three factors at five levels**

level	factor	A Inlet flow $Q_{inlet}$	B Branch diameter $d$	C Main pipe diameter $D$
1		0.068	0.01	0.015
2		0.274	0.015	0.02
3		0.616	0.02	0.03
4		1.164	0.025	0.04
5		1.711	0.03	0.05

The 25 sample point models were modelled and meshed sequentially according to the methods covered in Chapters 1 and 2 of this paper, and imported into Fluent software for simulation. In order to study the flow uniformity of the branch pipe and the heat transfer effect of the cold plate, the maximum flow deviation coefficient of the branch pipe and the maximum temperature, average temperature and maximum temperature difference of the cold plate are calculated according to the simulation results.

The maximum flow deviation coefficients of branch pipes at 25 sample points are analyzed, and the results are shown in Tab. 3. In this paper, the average temperature of the cold plate is analysed, the smaller the average temperature of the cold plate represents the better cooling effect of the cold plate. In Tab. 3, the smallest mean value of  $k_i$  represents the optimum heat transfer effect of the cold plate.

**Table 3. Data analysis of orthogonal test for maximum flow deviation coefficient of branch pipe**

Index	Inlet flow rate A	Branch pipe diameter B	Main pipe diameter C
K1	25.241	21.569	19.162
K2	23.883	23.761	22.924
K3	25.288	24.592	26.635
K4	25.292	26.581	27.397
K5	24.157	27.358	27.743
K1 mean	5.048	4.314	3.832
K2 mean	4.777	4.752	4.585
K3 mean	5.058	4.918	5.327
K4 mean	5.059	5.316	5.479
K5 mean	4.831	5.472	5.549
Extreme difference R	0.282	1.158	1.717
Excellent level	4.777 ( $i=2$ )	4.314 ( $i=1$ )	3.832 ( $i=1$ )
Primary and secondary factor	C > B > A		

Therefore, the overall flow uniformity of the stronger combination of structures for A2, B1, C1, the results are basically consistent with the previous single-factor working condition law. In terms of the degree of influence of the three factors on the maximum flow deviation coefficient of the branch pipe, the main pipe diameter has the greatest effect on the branch pipe flow uniformity, followed by the branch pipe diameter, and the inlet flow has the smallest degree of influence on the branch pipe flow uniformity.

The cold plate temperature distribution of 25 groups of sample experimental points is analyzed, and the results are shown in Tab. 4. The excellent level in Tab. 4 should be the minimum value of the average value of  $K_i$ , when the cold plate heat transfer effect is relatively optimal.

**Table 4. Data analysis of orthogonal test for average temperature of cold plates**

Index	Inlet flow rate A	Branch pipe diameter B	Main pipe diameter C
K1	318.88	258.56	255.93
K2	294.89	298.17	255.76
K3	279.49	259.87	280.25
K4	246.49	276.41	290.94
K5	228.97	269.71	285.84
K1 mean	63.78	51.71	51.15
K2 mean	58.98	59.63	51.19
K3 mean	55.90	51.97	56.05
K4 mean	49.30	55.28	58.19
K5 mean	45.79	53.94	57.17
Extreme difference R	17.99	7.66	7.04
Excellent level	45.79 (5)	51.71 (1)	51.15 (1)
Primary and secondary factor	A > B > C		

Therefore, the overall cold plate cooling effect of the optimal combination of heat transfer cooling structure for the A5, B1, C1, the results and the previous single-factor working condition law is basically consistent. In terms of the degree of influence of the three factors on the effect of cold plate heat transfer, the

inlet flow rate on the average temperature of the cold plate has the greatest effect, followed by the branch pipe diameter, the main pipe diameter on the average temperature of the cold plate has the smallest impact on the effect of the cold plate.

Throughout the experiments in this paper, it is found that the optimal structure combinations of comprehensive branch pipe flow uniformity are A2, B1, C1, and the optimal structure combinations of cooling effect of cold plate heat exchange are A5, B1, C1. Analyzing the difference between the two optimal structure combinations, it is found that only the data of group A is different, and since the inlet flow factor has the smallest impact on the branch pipe flow uniformity, the optimal branch pipe flow uniformity is selected under the premise of satisfying the cooling effect of cold plate heat exchange. The optimal combination of A5 ( $Q_{inlet}=1.711\text{kg/s}$ ), B1( $d=0.01\text{m}$ ), C1( $D=0.015\text{m}$ ) is chosen as the overall optimal combination for the whole test, which is consistent with the optimization results of the previous one-way analysis of variance method.

## 5. Conclusions

During our research process, we found that no other scholars have studied the flow distribution and heat transfer characteristics of  $2 \times 7$  Z parallel multi-branch cold plate. In this paper, the influence of different inlet flow rate, branch pipe diameter and main pipe diameter on the flow uniformity and cold plate heat transfer characteristics studied by using CFD numerical simulation software, and the conclusions are as follows:

(1) The non-uniformity of branch pipe flow increases with higher inlet flow rates, larger branch pipe diameters, and larger main pipe diameters.

(2) As the inlet flow rate increases, the temperature distribution of the cold plate improves, but the rate of temperature decrease slows down. The increase in branch pipe diameter has little effect on the cold plate's heat transfer, while a larger main pipe diameter results in a higher maximum temperature on the cold plate.

(3) A three-factor, five-level orthogonal test table was designed for inlet flow rate, branch pipe diameter and main pipe diameter, and the optimal overall structural combination of  $Q_{inlet}=1.711\text{ kg/s}$ ,  $d=0.01\text{ m}$ , and  $D=0.015\text{ m}$  was obtained, which is in line with the pattern of the results of the single-factor test in the previous section.

In summary, in a  $2 \times 7$  Z-type parallel multi-pipe group, branch pipe flow characteristics significantly impact the temperature distribution in cold plates. Therefore, real design must comprehensively consider both flow uniformity in branch pipes and the heat transfer effect of cold plates.

## Reference

- [1] Kubo, T., Ueda, T., On the characteristics of divided flow and confluent flow in headers, *Transactions of the Japan Society of Mechanical Engineers*, 12 (2008), pp. 802-809
- [2] Ahn, H., *et al.*, Flow distribution in manifolds for low Reynolds number flow, *Journal of Mechanical Science & Technology*, 12 (1998), pp. 87-95
- [3] Lee, J. K., Lee, S. Y., Distribution of two-phase annular flow at header-channel junctions, *Experimental Thermal & Fluid Science*, 28 (2004), pp. 217-222
- [4] Zhu, Z. Y., Experimental and visualization study on gas-liquid two phase flow character in distribution headers, *North China Electric Power University (Beijing) (in Chinese)* (2015)

- [5] Chen, F., *et al.*, An optimization method for uniform flow distribution in the manifold of server cabinet. *Energy Science & Engineering*, 9 (2021), pp. 390-401
- [6] Griffini, G., Gavriilidis, A., Effect of microchannel plate design on fluid flow uniformity at low flow rates. *Chemical Engineering & Technology: Industrial Chemistry - Plant Equipment - Process Engineering -Biotechnology*, 30 (2007), pp. 395-406
- [7] Kim, D., *et al.*, Effects of manifold geometries on flow uniformity in microchannel device, *Journal of Mechanical Science & Technology*, 25 (2011), pp. 3069-3074
- [8] Acrivos *et al.*, Flow distributions in manifolds, *Chemical Engineering Science*, 10 (1959), pp. 112-124
- [9] Amador, C., *et al.*, Flow distribution in different micro-reactor scale-out geometries and the effect of manufacturing tolerances and channel blockage. *Chemical Engineering Journal*, 101 (2004), pp. 379-390
- [10] Lee, J. K., Sang, Y. L., Distribution of two-phase annular flow at header–channel junctions, *Experimental Thermal and Fluid Science*, 28 (2004), pp. 217–222
- [11] Kim, N. H., Han, S. P., Distribution of air-water annular flow in a header of parallel flow heat exchanger. *International Journal of Heat & Mass Transfer*, 51 (2008), pp. 977-992
- [12] Fang, Y., *et al.*, Investigation on the transient thermal performance of a mini-channel cold plate for battery thermal management. *Journal of Thermal Science*, 30 (2021), pp.914-925
- [13] Shen, M., Gao, Q., Structure design and effect analysis on refrigerant cooling enhancement of battery thermal management system for electric vehicles. *Journal of Energy Storage*, 32 (2020), 101940
- [14] Hosseini S M *et al.*, Classification of turbulent jets in a T-junction area with a 90-deg bend upstream. *International Journal of Heat and Mass Transfer*, 51 (2008), pp.2444-2454
- [15] Gong, Z., *et al.*, A study of the effects of the micro-channel cold plate on the cooling performance of battery thermal management systems. *Thermal Science*, 26 (2022), pp.1503-1517
- [16] Sharma, M. K., *et al.*, Flow Distribution of Multiphase Flow in Parallel Channels. *Handbook of Multiphase Flow Science and Technology*. Singapore: Springer Nature Singapore, 2023, pp.1241-1277

Submitted: 10.09.2024.

Revised: 05.11.2024.

Accepted: 12.11.2024.